Triple-Helix Formation and Cooperative Binding by Oligodeoxynucleotides with a 3′–3′ Internucleotide Junction

Brian C. Froehler,* Terry Terhorst, Jeng-Pyng Shaw, and Sarah N. McCurdy

Gilead Sciences Inc., 346 Lakeside Drive, Foster City, California 94404

Received August 13, 1991; Revised Manuscript Received November 13, 1991

ABSTRACT: Triple-helix formation by oligodeoxynucleotides in a sequence-specific manner is limited to polypurine tracts of duplex DNA. To increase the number of biologically relevant targets for triple-helix formation, we have utilized oligodeoxynucleotides containing a 3′–3′ internucleotide junction to allow for binding to opposite strands of duplex DNA. Molecular modeling was used to aid in the design of the xylose dinucleoside linker **1** that is rigid and minimizes the number of conformers to minimize the entropy of binding. Thermal denaturation studies show that a 3′–3′-linked oligodeoxynucleotide, bearing nine nucleotides on each side of the linker, has a higher T_m (47.6 °C) than that of a 21-mer binding to a single polypurine tract (45.3 °C). Binding domain minimization studies and sequence-specific alkylation of a target duplex demonstrate a high degree of cooperativity between the two triple-helix binding domains, thus allowing for an increase in the number of biologically relevant targets for triple-helix formation.

Sequence-specific triple-helix formation by ODN's[1] (Moser & Dervan, 1987) has therapeutic potential as an approach to inhibiting gene expression and has therefore become an area of intense research (Maher et al., 1989, 1990; Praseuth et al., 1988; François et al., 1989). Triple-helix-forming ODN's incorporating Fe/EDTA functionality are capable of cleaving genomic DNA at a single specific target site (Strobel et al., 1988), and triple-helix-forming ODN's have also been used to inhibit c-myc expression in vitro (Cooney et al., 1988). The third strand of a triple helix lies in the major groove of the duplex (Arnott et al., 1976) and allows for the possibility of binding to both strands of the duplex by crossing the major groove. In an effort to increase the number of biologically relevant targets for triple-helix formation, ODN's with inverted polarity (with one 3′–3′ linkage) have been used to allow for binding to opposite strands of duplex DNA (Horne & Dervan, 1990; McCurdy et al., 1991) (Figure 1a). Alternate-strand triple-helix formation, utilizing 1,2-dideoxyribose (**2**) as a linker element, has been reported (Horne & Dervan, 1990), and our preliminary results, utilizing other linkers, have also been described (McCurdy et al., 1991). More recently, a report has described triple-helix formation with both 3′–3′- and 5′–5′-linked ODN's. An ODN with inverted polarity and the proper linker element is able to switch from one purine tract to another on opposite strands of the duplex target and has been termed a "switchback" ODN (McCurdy et al., 1991). This allows for binding to target sequences consisting of a polypurine tract followed by a polypyrimidine tract and increases the number of target sites available for triple-helix formation in duplex DNA.

The goal of this work was to determine if a switchback ODN, with the proper linker element, is able to bind to duplex DNA with equal affinity as that of a 3′–5′ ODN binding to a single polypurine tract. To answer this question, T_m analysis was used. Thermal denaturation of triple helices has been reported by a number of workers (Pilch et al., 1990a,b; Shea et al., 1990). It has also been shown that the T_m of a triple helix is pH dependent when the third strand contains cytosines (Plum et al., 1990); thus the T_m at various pH values was used to compare the different switchback ODN linkers to each other as well as to 3′–5′ ODN's.

Molecular modeling was used to assist in the design of a linker element that minimizes steric crowding and is sufficiently rigid to minimize the entropy of binding. The result is the xylose linker **1** (Figure 2a) that allows for recognition of two separate binding domains with a high degree of cooperativity. Switchback ODN's derived from linker **1** have a much higher T_m than switchback ODN's derived from the previously reported linkers (Horne & Dervan, 1990; McCurdy et al., 1991), and the results reported below demonstrate that the switchback ODN's bind at least as well as an ODN with normal 3′–5′ linkages. The T_m of an 18 nucleotide (nt) long switchback ODN is greater than that of a 21-mer recognizing a single polypurine tract with a similar sequence context. The high degree of cooperativity with this ODN is demonstrated by a sequence-specific alkylation experiment utilizing switchback ODN's containing a large and a small binding domain.

Materials and Methods

Synthesis of Deoxyoligonucleotides and Diol Linkers. Oligodeoxynucleotides were prepared on a Milligen/Biosearch 8750 DNA synthesizer by H-phosphonate chemistry (Froehler et al., 1986) and purified by preparative polyacrylamide gel electrophoresis. Synthesis of ODN's containing a 3′–3′ junction was carried out with the first nucleoside attached to the CPG via the 5′-hydroxyl (van de Sande et al., 1988); 3′-DMT-protected nucleoside 5′-H-phosphonates were then coupled in standard fashion to the point of the linker, and the linker was then incorporated into the ODN followed by coupling with 5′-DMT-protected nucleoside 3′-H-phosphonates to complete the sequence (Horne & Dervan, 1990).

Dimethoxytrityl-protected 1,3-propanediol (Seela & Kaiser, 1987) and 1,2-dideoxyribose (Horne & Dervan, 1990) were prepared and phosphitylated by standard procedures (Marugg et al., 1986). 5′-Dimethoxytrityl-protected 2′-deoxy-xylosofuranosylthymine (**4**) was prepared from the anhydro-

[1] Abbreviations: ODN, oligodeoxynucleotide; T_m, thermal denaturation; nt, nucleotides; nbp, null base pairs; DCA, dichloroacetic acid; TEAB, triethylammonium bicarbonate.

0006-2960/92/0431-1603$03.00/0

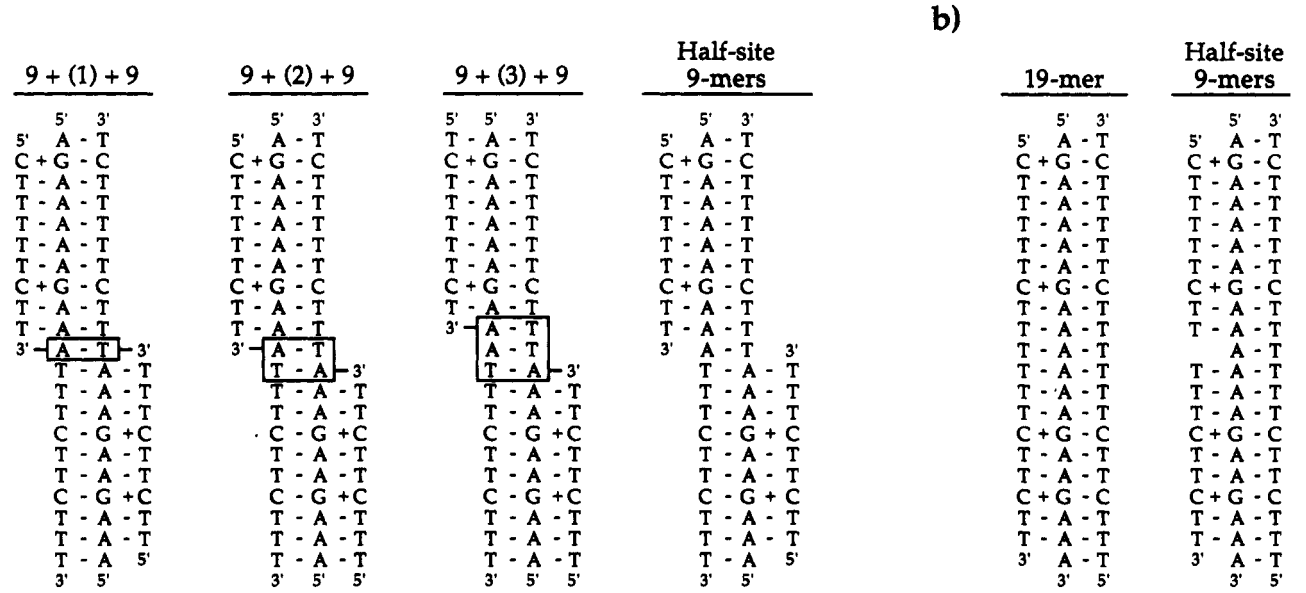

FIGURE 1: (a) Duplex and third-strand sequences for 9 + 9 switchback ODN's. The duplex is kept constant, and the third-strand sequences differ in the number of null base pairs spanned upon binding. The box represents null base pairs. The two 9-mer half-sites are the same sequences as the ODN spanning 1 nbp without a linker element. (b) Duplex and third-strand sequence for single polypurine tract binding studies and two 9-mer half-site ODN's spanning 1 nbp as above.

nucleoside of 5′-DMT-thymidine (Secrist, 1975) followed by alkaline hydrolysis.

Synthesis of Ether-Linked Dinucleoside H-Phosphonate (1). NaH (400 mg, 36 mmol, 60% dispersion in mineral oil) was washed with anhydrous THF (2 × 10 mL) and suspended into 20 mL of anhydrous THF, and **4** (545 mg, 1.0 mmol) was added with stirring under Ar. After evolution of H_2 had ceased, NaI (150 mg, 1.0 mmol) and α,α'-*o*-dibromoxylene (130 mg, 0.49 mmol) were added, and the reaction mixture was stirred at 40 °C for 18 h. The reaction mixture was cooled to room temperature, slowly quenched with saturated aqueous $NaHCO_3$, evaporated to a gum, taken up in CH_2Cl_2 (50 mL), washed with $NaHCO_3$ (2 × 50 mL), dried over Na_2SO_4, and evaporated. Purification by flash chromatography on silica gel using a MeOH/CH_2Cl_2 gradient (0–5%) yielded 549 mg (0.46 mmol, 92% yield) of symmetrical dimer **5**. **5** (549 mg, 0.46 mmol) was dissolved into 10 mL of MeOH/CH_2Cl_2 (1/1), and to this was added, with stirring, 10 mL of 10% DCA in MeOH/CH_2Cl_2 (1/1). After 25 min the reaction was quenched by the addition of saturated aqueous $NaHCO_3$ (~15 mL) and transferred to a separatory funnel with 40 mL of CH_2Cl_2, the layers were separated, and the organic layer was washed with saturated $NaHCO_3$ (2 × 50 mL), dried over Na_2SO_4, and evaporated to yield a mixture of **5** and **6**. The crude material was coevaporated from anhydrous pyridine (2 × 20 mL), taken up in 10 mL of Pyr/CH_2Cl_2 (1/1), added to 10 mL of a 0.5 M solution of 2-chloro-4*H*-1,3,2-benzodioxaphosphorin-4-one in Pyr/CH_2Cl_2 (1/1) at room temperature, stirred for 15 min, and poured into 75 mL of aqueous TEAB (1 M, pH = 8.5). The H-phosphonate was extracted into CH_2Cl_2 (50 mL), dried over Na_2SO_4, evaporated, purified by flash chromatography, and converted to the DBU salt to yield 177 mg (0.16 mmol, 35% from **5**) of **1**.

Thermal Denaturation. T_m values were determined by a first-derivative plot of absorbance vs temperature. Thermal denaturation was carried out using a Gilford Response II temperature-controlled spectrophotometer, and absorbance was monitored at 260 nm. The rate of heating was 0.25 °C/min from 15 to 75 °C. The extinction coefficients for the ODN's were calculated (Fasman, 1976), and the final concentration of all three strands was ~2 μM. To approximate physiological conditions, the buffer was prepared from 140 mM KCl/5 mM Na_2HPO_4/5 mM $MgCl_2$ and brought to the appropriate pH with dilute phosphoric acid. Prior to every T_m measurement the buffers were degassed with Ar, and the pH was adjusted to the exact pH (±0.01). T_m curves for all experiments were sharp biphasic transitions, the first transition due to third-strand denaturation and the second transition due to duplex denaturation. The total hypochromicity for the triple-helix to duplex to single-strand denaturation was 24–28%. Approximately 40% of the total hypochromicity was due to third-strand denaturation and the remaining ~60% due to duplex denaturation.

Triple-Helix Alkylation. Sequence-specific switchback ODN alkylation was carried out on a 430-bp restriction fragment at 37 °C in 25 mM MOPS/140 mM KCl/10 mM NaCl/1 mM $MgCl_2$/1 mM spermine tetrahydrochloride/1 μg of salmon sperm DNA at pH = 7.2. Aliquots were removed at the time points indicated (hours), quenched with pyrrolidine, heated at 95 °C for 10 min, and evaporated. Electrophoresis was with a 7 M urea/6% acrylamide gel at 60 W for 1.5 h.

Molecular Model. A model of the switchback triple-helix complex was constructed on a Silicon Graphics Personal Iris Workstation utilizing Biodesign/Biograf v. 2.10 software. To construct the switchback triple helix, which contains an underlying duplex with a polypurine tract followed by a polypyrimidine tract, two triple-helix structures were docked to each other. As a starting point for the triple helix, the fiber defraction coordinates of Arnott (1976) were used to construct the triple helix $d(T)_7$·$d(A)_7$·$d(T)_7$ which was minimized (Drieden force field) and duplicated. The duplicate was rotated 180° about the *x*-axis and moved vertically along the *y*-axis, resulting in a disjointed triple helix in which the 3′ ends of the two third strands were abutted to each other. The 3′-terminal nucleoside of each of the third strands was removed, and the two triple helices were docked such that the purine strand of one duplex formed a 5′–3′ internucleotide junction with the pyrimidine strand of the other duplex, thus generating a switchback structure with 2 null base pairs (nbp). The configuration of the 3′-terminal hydroxyls of the third strands was inverted to generate xylose sugars, and this

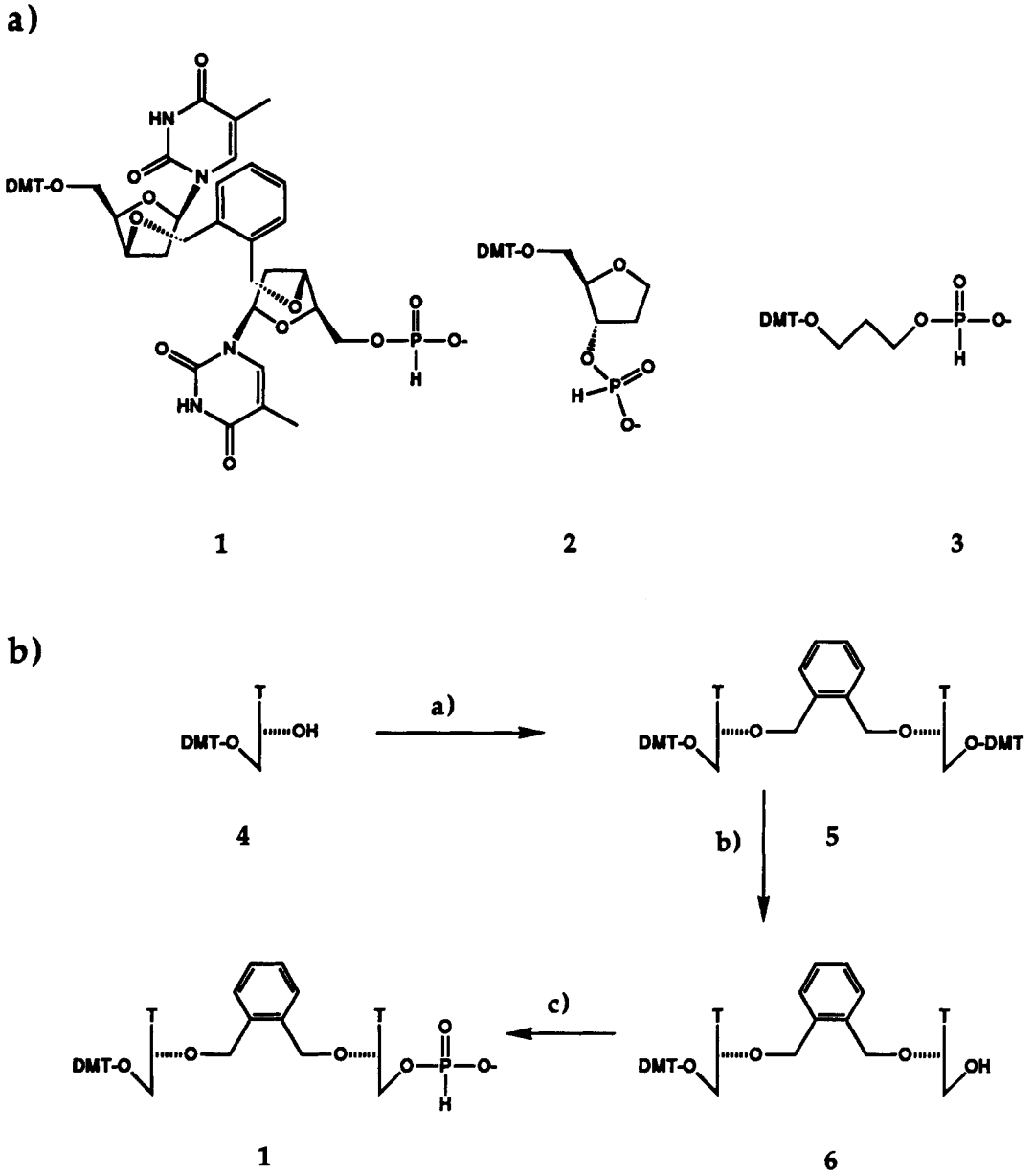

FIGURE 2: (a) Structure of switchback linkers: **1** is the 3′–3′ xylose dimer, **2** is derived from 1,2-dideoxyribose, and **3** is derived from 1,3-propanediol. (b) Synthesis of ether-linked dinucleoside H-phosphonate **1**: (a) NaH/α,α'-*o*-dibromoxylene/THF, 40 °C; (b) 5% DCA in CH_2Cl_2/MeOH (1/1); (c) 2-chloro-4*H*-1,3,2-benzodioxaphosphorin-4-one in pyridine/CH_2Cl_2 (1/1).

structure was used to model the xylose linker **1**. To model the diol linker elements (**2** and **3**), the 3′-terminal nucleoside of one of the third strands was removed, to generate a structure with 3 nbp, and the 3′-hydroxyls were left in the ribose configuration.

RESULTS

Figure 1a shows a 21-mer duplex target that contains two separate polypurine binding domains, one on each strand of the duplex DNA. The target duplex is asymmetric, allowing only one binding orientation. The corresponding switchback ODN's have a 3′–3′ internucleotide junction and thus two 5′ ends. The length of the ODN's was 18 bases, 9 bases recognizing each binding domain separated by the linker element (referred to as a 9 + 9 switchback). Molecular modeling reveals that the target duplex contains base pairs that do not participate in Hoogsteen base-pair interactions with the third strand; these base pairs are spanned by the linker element and are referred to as null base pairs (nbp, indicated by a box in Figure 1a). For these studies the duplex target was kept constant, and therefore three different third-strand sequences were synthesized to determine the effect of differing numbers of nbp (1–3; Figure 1a). The ether-linked dinucleoside (**1**) was synthesized from α,α'-*o*-dibromoxylene and contains a DMT protecting group at one of the 5′-hydroxyls and a H-phosphonate at the other 5′-hydroxyl (Figure 2a). Incorporation of this dinucleoside into the ODN provided the 3′–3′ junction, with the dinucleoside becoming the first base in each binding domain. Ether-linked dinucleoside linker **1** was used to synthesize two ODN sequences that target the same duplex and span 1 and 2 nbp [9 + (1) + 9 and 9 + (2) + 9, respectively; Figure 1a]. The diol linker elements (**2** and **3**) were used to synthesize two ODN sequences that target this same duplex and span 2 and 3 nbp [9 + (2) + 9 and 9 + (3) + 9, respectively; Figure 1a]. Also shown in Figure 1a are two half-site 9-mers, separated by 1 nbp. These ODN's were used to assess the relative cooperativity of binding by the 9 + (1) + 9 switchback ODN compared to ODN's in the absence of the linker element. To compare the cooperativity of binding between the switchback ODN's relative to an ODN binding

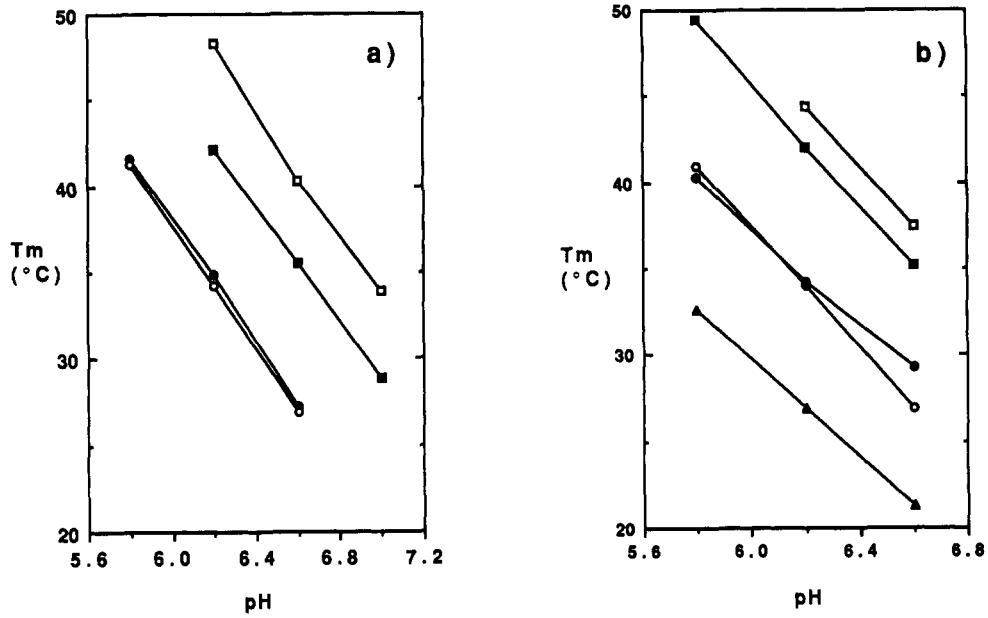

FIGURE 3: T_m vs pH plot of switchback ODN's at a concentration of ~2 μM. The rate of heating was 0.25 °C/min in 140 mM KCl/5 mM Na_2HPO_4/5 mM $MgCl_2$ at the pH values indicated. (a) (□) 9 + (2) + 9 with linker **1**; (■) 9 + (1) + 9 with linker **1**; (○) 9 + (2) + 9 with linker **2**; (●) 9 + (2) + 9 with linker **3**. (b) (□) 15 + (2) + 3 with linker **1**; (■) 12 + (2) + 6 with linker **1**; (●) 15-mer control; (○) 15 + (2) + 3 with linker **3**; (▲) 12 + (2) + 6 with linker **3**.

Table I: T_m of 9 + 9 Switchback ODN's at pH = 6.20

ODN linker	T_m (°C)		
	1 nbp	2 nbp	3 nbp
1	42.1	47.6	nd[a]
2	nd	34.2	28.9
3	nd	34.9	29.1

[a] nd, not determined.

to a single polypurine tract, a 19-mer and two half-site 9-mers, with the same sequence but no inversion of polarity, were also synthesized. Figure 1b shows the 21-mer duplex target that contains one polypurine binding domain and the 19-mer third-strand ODN, as well as the two half-site 9-mers separated by 1 nbp. The T_m of these ODN's and the breadth of the transition of the thermal denaturation were used as measurements of the relative degree of cooperativity between the switchback ODN and an ODN binding to a single polypurine tract.

To approximate physiological conditions, thermal denaturation analysis was carried out in 140 mM KCl/5 mM Na_2HPO_4/5 mM $MgCl_2$. Figure 3a shows the T_m vs pH plot for the switchback ODN derived from the xylose linker **1** targeting the duplex spanning 1 and 2 nbp and the diol-derived switchback ODN's (**2** and **3**) targeted to 2 nbp. The most stable triple helix is derived from linker **1** targeting 2 nbp, and the second most stable is derived from the same linker targeting 1 nbp (Table I). There is very little difference in T_m of the two diol-derived switchback ODN's targeted to 2 and 3 nbp (Table I). All of the triple-helix complexes show a sharp pH dependence with a slope of −16 to −19 °C/pH unit (Figure 3a). As expected, in all cases, the T_m of the duplex (57.6 °C ± 0.3) showed no pH dependency.

At pH = 6.6 the 9 + (1) + 9 switchback ODN derived from the xylose linker **1** has a T_m of 35.6 °C, the 9 + (2) + 9 switchback ODN has a T_m of 41.2 °C, and the 19-mer, shown in Figure 1b, has a T_m of 39.5 °C. The T_m curves for these three ODN's are shown in Figure 4a, and the triple-helix transitions for all of these ODN's are comparable in breadth and slope, indicating approximately equal cooperativity. The T_m curves for the combination of half-site 9-mers (Figure 1) gave very broad triple-helix transitions (Figure 4b), and the T_m of both complexes was <20 °C at pH = 5.5.

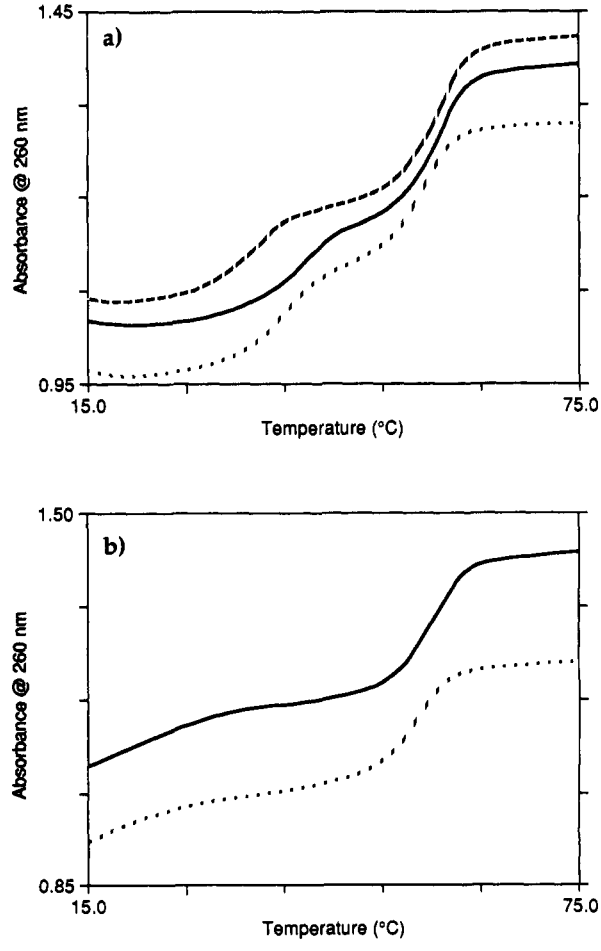

FIGURE 4: (a) T_m curves for switchback ODN's and 19-mer binding to a single polypurine tract at pH = 6.6: (---) 9 + (1) + 9 switchback ODN; (—) 9 + (2) + 9 switchback ODN; (···) 19-mer. (b) T_m curves for half-site 9-mer ODN's at pH = 5.5: (—) binding to switchback duplex (Figure 1a); (···) binding to single polypurine tract (Figure 1b).

Table II: T_m of Length Standards at pH = 6.20

ODN	T_m (°C)	ODN	T_m (°C)
14-mer	34.9	18-mer	43.9
15-mer	39.4	19-mer	44.4
16-mer	42.1	20-m34	44.8
17-mer	43.4	21-mer	45.3

14-mer: 5′-TTTCTTTCTCTTCT
15-mer: 5′-TTTCTTTCTCTTCTT
16-mer: 5′-TTTCTTTCTCTTCTTT
17-mer: 5′-TTTCTTTCTCTTCTTTT
18-mer: 5′-TTTCTTTCTCTTCTTTTT
19-mer: 5′-TTTCTTTCTCTTCTTTTTT
20-mer: 5′-TTTTCTTTCTCTTCTTTTTT
21-mer: 5′-TTTTTCTTTCTCTTCTTTTTT

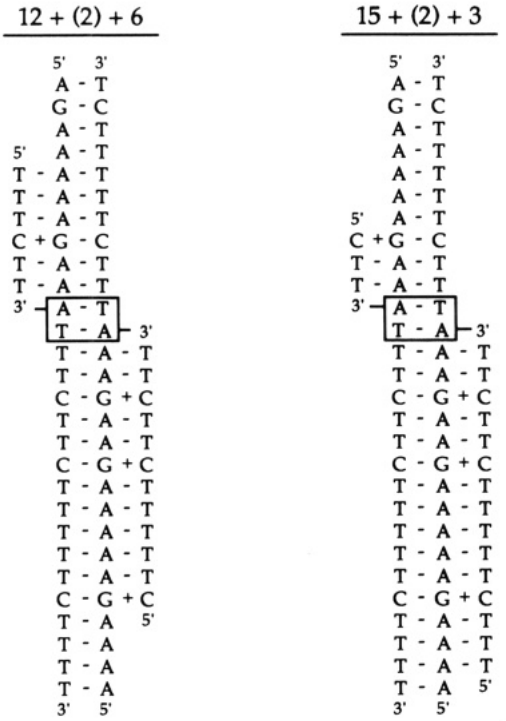

FIGURE 5: Binding domain minimization sequences for linkers **1** and **3**. The length of the ODN's is 18 nt long with a primary (15 or 12 nt long) and secondary (3 or 6 nt long) binding domain. Both third-strand sequences span 2 nbp upon binding to the target duplex.

To determine how the range of T_m values reported above compare to ODN's binding to a single polypurine tract, a series of length standards were prepared. ODN's 14 through 21 bases in length, containing four cytosines in each, had T_m values that range from 34.9 (14-mer) to 45.3 (21-mer) at pH = 6.2 and a slope of −16 to −17 °C/pH unit (Table II). The T_m values shown in Tables I and II show that the T_m's of the 9 + 9 switchback ODN's (**1**–**3**) range from that of a 14-mer to greater than that of a 21-mer.

The position of the 3′–3′ junction was next shifted to test if the junction was required to be in the middle of the ODN. Binding domain minimization studies were carried out utilizing linkers **1** and **3** to determine how small a binding domain is required to maintain binding affinity. The total length of the switchback ODN's remained 18 nt, but the two separate binding domains were asymmetric in length, generating a switchback ODN with a primary (15 or 12 nt long) and secondary (3 or 6 nt long) binding domain (Figure 5). The T_m of the 15 + (2) + 3 switchback ODN derived from **1** is 10 °C higher than the 15-mer control, which has a T_m similar to the 15 + (2) + 3 switchback ODN utilizing linker **3** (Figure 3b). With both linkers the T_m of the 12 + (2) + 6 switchback ODN was lower than the corresponding 15 + (2) + 3 switchback ODN, although the ΔT_m utilizing linker **1** was much less than the ΔT_m utilizing linker **3** (Figure 3b).

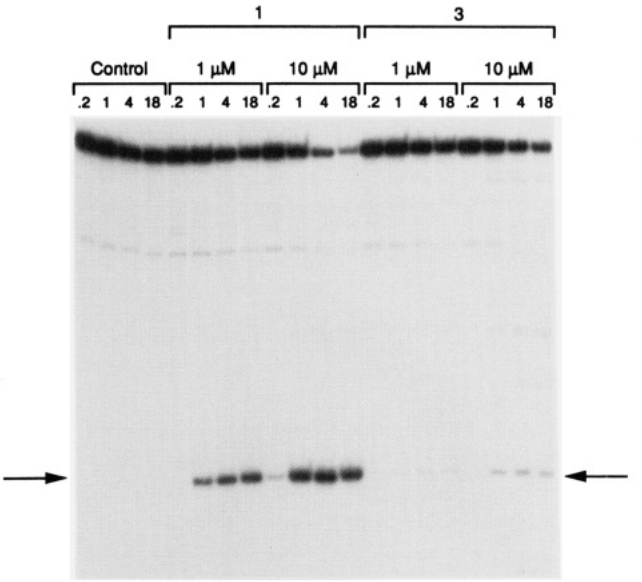

FIGURE 6: Autoradiogram derived from denaturing PAGE analysis of 14 + (2) + 3 switchback ODN alkylation of the 430-bp restriction fragment: (a) no ODN control; (b) linker **1** at 1 and 10 μM; (c) linker **3** at 1 and 10 μM. The arrow indicates the cleavage product.

To further assess the degree of the interaction of the secondary binding domain, an alkylation experiment was carried out. N^4,N^4-Ethano-5-methyl-2′-deoxycytidine has been shown to alkylate the N-7 of guanosine in a sequence-specific manner when incorporated into a triple-helix-forming ODN, which, upon pyrrolidine and heat treatment, leads to cleavage of the target strand (Shaw et al., 1991). The 14 + (2) + 3 switchback ODN's derived from linkers **1** and **3** were prepared in which the terminal cytosine, of the secondary binding domain, was substituted with N^4,N^4-ethano-5-methyl-2′-deoxycytidine. The results shown in Figure 6 demonstrate that the switchback ODN derived from linker **3** gives a very low yield of alkylation (<5% after 18 h at 10 μM) while the switchback ODN derived from linker **1** gives a very high yield of alkylation (>85% after 18 h at 10 μM).

Discussion

Thermal denaturation analysis of switchback ODN's indicates a large difference in the thermal stability of the complex depending on the linker element used (Figure 3a, Table I). Surprisingly, there is very little difference in T_m values between linkers **2** and **3**; a previous report suggested a somewhat larger difference based upon affinity cleavage analysis (approximately 3-fold; Horne & Dervan, 1990). Conversely, the T_m of the xylose switchback ODN derived from linker **1** is much higher than the diol-derived switchback ODN's ($\Delta T_m \sim 13$ °C).

A switchback ODN can be envisioned as an ODN with inverted polarity and with the replacement of the normal phosphate diester of a 3′–5′ ODN by the linker element. T_m analysis of ODN's binding to a single polypurine tract provides a comparison of the cooperativity of a normal 3′–5′ ODN relative to the switchback ODN's. The T_m curves in Figure 4a show that the switchback ODN's derived from linker **1** have the same breadth of transition as the control 19-mer binding to a single polypurine tract. This indicates that the cooperativity of binding of the switchback ODN is approximately equal to that of a normal 3′–5′ ODN. Conversely, the two half-site 9-mers, separated by 1 nbp, show a very broad

transition (Figure 4b), and the T_m's, at pH = 5.5, are well below the T_m of the switchback ODN at pH = 6.6. Cooperativity of binding to duplex DNA has been shown between contiguous 9-mers in the absence of an intervening nbp (Strobel & Dervan, 1989). The results presented above with the two 9-mer half-sites indicate very little, if any, cooperativity between the two binding domains. These results suggest that the effect observed by Strobel and Dervan may be due to stacking interactions that are disrupted by an intervening nbp.

All switchback ODN's tested are 18 nt long, and if these ODN's demonstrate equal cooperativity to a 3′–5′ ODN binding to a single polypurine tract, the T_m of the switchback ODN should be similar to that of the 18-mer. The most striking aspect of the data presented in Tables I and II is that the switchback ODN derived from **1** (an 18-mer), when hybridized to a target spanning 2 nbp, has a higher T_m than that of a 21-mer, containing the same number of cytidine residues as the switchback ODN's, targeted to a single polypurine tract. This result demonstrates that the cooperativity of binding by the switchback ODN is greater than or equal to that of a 3′–5′ ODN and suggests that the preferred linker, **1**, is superior to the phosphate diester linkage of a 3′–5′ ODN for triple-helix binding in terms of steric and entropic considerations. Conversely, the switchback ODN's derived from linkers **2** and **3** have a T_m similar to that of a 14-mer (Tables I and II), indicating a lower degree of cooperativity between the two binding domains.

For switchback recognition to be of major utility, it is necessary to bind to sequences with small and large binding domains; this increases the number of target sites available for triple-helix formation but requires a high degree of cooperativity between the two triple-helix binding domains. The results presented in Figure 3b indicate that linker **1** leads to a very strong interaction of the secondary binding domain with the target duplex and demonstrate a high degree of cooperativity between the primary and secondary binding domains. The importance of the interaction from the secondary binding domain, with an ODN derived from linker **1**, was confirmed with a 15 + (2) + 3 switchback ODN containing two mismatches. The terminal two bases of the secondary binding domain (3 nt long; Figure 5) were transposed to generate a double mismatch, and the T_m of this ODN was 9 °C lower than the 15 + (2) + 3 with the proper base pairs for triple-helix formation and 1 °C higher than the 15-mer control (data not shown). This confirms the importance of interaction of the secondary binding domain utilizing linker **1**. The data shown in Figure 3b also indicate that there is very little, if any, interaction of the secondary binding domain utilizing linker **3**.

Alkylation of a target duplex with an asymmetric switchback ODN is a very sensitive method for measuring the interaction of the secondary binding domain utilizing the different linkers. It has previously been shown that proper base-pair interaction of the third strand is required for duplex DNA alkylation (Shaw et al., 1991). The rate and yield of alkylation of the switchback ODN derived from linker **1** (Figure 6) is comparable to an 18-mer ODN binding to a single polypurine tract (Shaw et al., 1991) and demonstrates that the two binding domains are cooperative. The switchback ODN derived from linker **3** showed very little alkylation of the target duplex (Figure 6), which suggests that there is very little interaction of the secondary binding domain. These results are consistent with the T_m data (Figure 3b) and show definitively that the secondary binding domain of the 14 + (2) + 3 switchback ODN derived from linker **1** is interacting strongly with the target duplex.

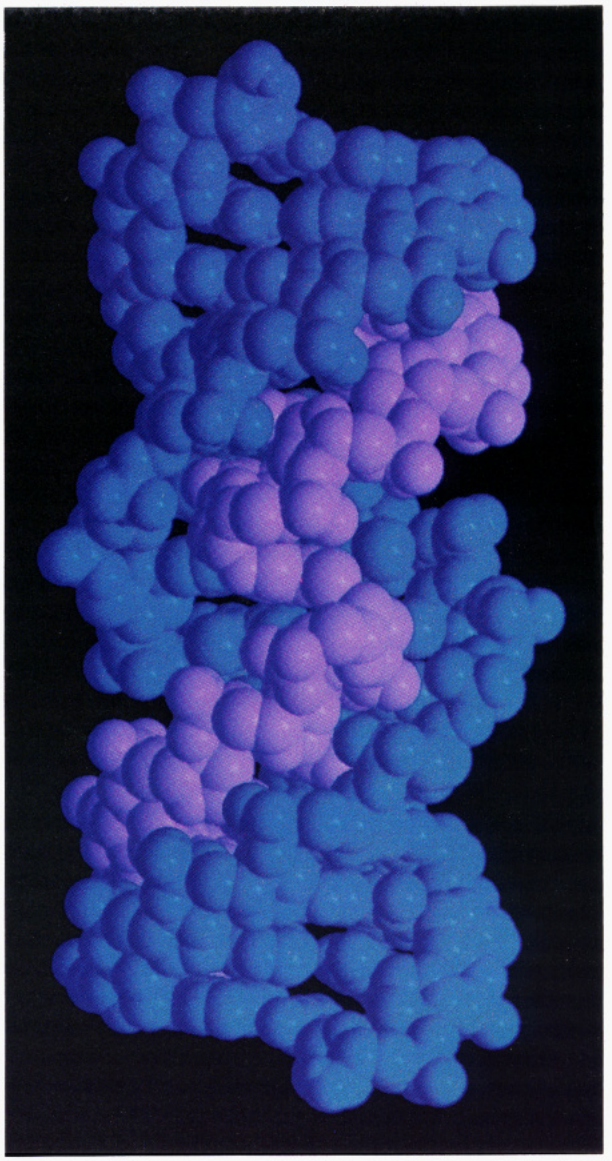

FIGURE 7: Molecular model of the switchback triple-helix complex incorporating linker **1** spanning 2 nbp.

The high degree of cooperativity and increased stability observed with the switchback ODN derived from linker **1** are likely due, in part, to entropic considerations. The switchback ODN derived from **1**, upon hybridization, places the two sugars adjacent to one another, and the linker spans the major groove along the *x*-axis, resulting in a compact and compressed structure (Figure 7). The dinucleoside linker element **1** is highly preorganized for binding so that when one of the nucleosides of the dimer binds to the target, the other nucleobase is located in close proximity for binding to the target on the opposite strand. All the substituents of the dinucleoside dimer are on the β-face of the sugar, and due to steric interactions, the freedom of rotation about the linker axis (defined from C-3′ to C-3′) is limited (Figure 7).

Conclusions

The data presented here clearly demonstrate that both binding domains of the switchback ODN are binding to the target duplex. Thermal denaturation analysis does not address the question of specificity of binding in the presence of alternate duplex DNA sequences. We previously have shown, by DNase footprint analysis, that switchback ODN's do bind specifically to the target sequence contained within a 327-bp

restriction fragment and that binding is to both domains (McCurdy et al., 1991). This is also supported by earlier studies utilizing DNA affinity cleavage analysis of a switchback ODN derived from the diol linker **2** (Horne & Dervan, 1990).

The 3′–3′ switchback ODN's were designed to overcome some of the limitations of triple-helix code recognition by binding to opposite strands of duplex DNA. Molecular modeling was employed to aid in the deisgn of a rigid linker element that enhances binding of the third strand and shows a high degree of cooperativity. High binding affinity is maintained when the target duplex is asymmetric and therefore allows for targeting of a greater diversity of sites within duplex DNA.

ACKNOWLEDGMENTS

We thank Sylvia Wu and David Sweedler for synthesis of the mononucleosides and the derivatized solid supports and especially thank Dr. Mark Matteucci for many valuable discussions.

REFERENCES

Arnott, S. A., Bond, P. J., Selsing, E., & Smith, P. J. C. (1976) *Nucleic Acids Res.*, 2459.

Cooney, M., Czernuszewicz, G., Postel, E. H., Flint, S. J., & Hogan, M. E. (1988) *Science 241*, 456.

Fasman, G. D., Ed. (1976) *Handbook of Biochemistry and Molecular Biology, Vol. I, Nucleic Acids*, p 589, CRC Press, Cleveland, OH.

François, J.-C., Saison-Behmoaras, T., Barbier, C., Chassignol, M., Thuong, N. T., & Helene, C. (1989) *Proc. Natl. Acad. Sci. U.S.A. 86*, 9702.

Froehler, B., Ng, P., & Matteucci, M. (1986) *Nucleic Acids Res. 14*, 5399.

Horne, D. A., & Dervan, P. B. (1990) *J. Am. Chem. Soc. 112*, 2435.

Maher, L. J., Wold, B. J., & Dervan, P. B. (1989) *Science 245*, 725.

Maher, L. J., Dervan, P. B., & Wold, B. J. (1990) *Biochemistry 29*, 8820.

Marugg, J. E., Tromp, M., Kuyl-Yeheskiely, E., van der Marel, G. A., & van Boom, J. H. (1986) *Tetrahedron Lett. 27*, 2661.

McCurdy, S., Moulds, C., & Froehler, B. (1991) *Nucleosides Nucleotides 10*, 287.

Moser, H. E., & Dervan, P. B. (1987) *Science 238*, 645.

Ono, A., Chen, C.-N., & Kan, L.-S. (1991) *Biochemistry 30*, 9914.

Pilch, D. S., Levenson, C., & Shafer, R. H. (1990a) *Proc. Natl. Acad. Sci. U.S.A. 87*, 1942.

Pilch, D. S., Brousseau, R., & Shafer, R. H. (1990b) *Nucleic Acids Res. 18*, 5743.

Plum, G. E., Park, Y.-W., Singleton, S. F., Dervan, P. B., & Breslauer, K. J. (1990) *Proc. Natl. Acad. Sci. U.S.A. 87*, 9436.

Praseuth, D., Perrouaolt, L., Le Doan, T., Chassignol, M., Thuong, N., & Helene, C. (1988) *Proc. Natl. Acad. Sci. U.S.A. 85*, 1349.

Secrist, J. A. (1975) *Carbohydr. Res. 42*, 379.

Seela, F., & Kaiser, K. (1987) *Nucleic Acids Res. 15*, 3113.

Shaw, J.-P., Milligan, J., Krawczyk, S., & Matteucci, M. (1991) *J. Am. Chem. Soc. 113*, 7765.

Shea, R. G., Ng, P., & Bischofberger, N. (1990) *Nucleic Acids Res. 18*, 4859.

Strobel, S. A., & Dervan, P. B. (1989) *J. Am. Chem. Soc. 111*, 7286.

Strobel, S. A., Moser, H. E., & Dervan, P. B. (1988) *J. Am. Chem. Soc. 110*, 7927.

van de Sande, J. H., Ramsing, N. B., Germann, M. W., Elhorst, W., Kalisch, B. W., Kitzing, E. V., Pon, R. T., Clegg, R. C., & Jovin, T. M. (1988) *Science 241*, 551.